Damping of Structural Vibrations with Piezoelectric Materials and Passive Electrical Networks

Nesbitt W. Hagood*, Andreas von Flotow+
Space Engineering Research Center
Massachusetts Institute of Technology
Bldg. 37 Rm. 341
Cambridge, Massachusetts 02139
(617) 253-8365 (617) 253-4865

Abstract

This paper investigates the possibility of dissipating mechanical energy with piezoelectric material shunted with passive electrical circuits. The effective mechanical impedance for the piezoelectric element shunted by an arbitrary circuit is derived. The shunted piezoelectric is shown to posses frequency dependant stiffness and loss factor which are dependant on the shunting circuit. The generally shunted model is specialized to two cases: the case of a resistor alone and that of a resistor and inductor. For resistive shunting, the material properties have frequency dependance similar to viscoelastic materials but with much higher stiffness and temperature stability. Shunting with a resistor and inductor introduces an electrical resonance, which can be optimally tuned to structural resonances in a manner analogous to a mechanical vibration absorber. Techniques for analyzing systems which incorporate these shunting cases are presented and applied to a cantilevered beam experiment. The experimental results for both the resistive and resonant shunting circuits validate the shunted piezoelectric damping models.

Nomenclature

$\mathbf{A}$	=	diagonal matrix of cross sectional areas of piezoelectric bar
C	=	generic capacitance
C_{pi}	=	inherent capacitance of the piezoelectric shunted in the i^{th} direction
d_{ij}	=	piezoelectric material constant relating voltage in i^{th} direction to strain in j^{th} direction
$\mathbf{D}$	=	vector of electrical displacements (charge/area)
E	=	elastic modulus of material
$\mathbf{E}$	=	vector of electric fields (volts/meter)
g	=	real nondimensional frequency ratio = ω/ω_n
$\mathbf{I}$	=	vector of external applied currents
K	=	modal stiffness
k_{ij}	=	material electromechanical coupling coefficient
K_{ij}	=	generalized electromechanical coupling coefficient
$\mathbf{L}$	=	diagonal matrix of lengths of piezoelectric bar
L	=	generic inductor
M	=	modal mass
r	=	dissipation tuning parameter ($RC^s_p\omega_n$)

* Graduate Research Assistant, Department of Aeronautics and Astronautics
+ Assistant Professor, Department of Aeronautics and Astronautics

R	=	generic resistance
s	=	Laplace parameter
s^E	=	piezoelectric material compliance matrix at constant field
S	=	vector of material strains
T	=	vector of material stresses
U_i	=	potential energy of element i
v	=	velocity
V	=	voltage
x^{ST}	=	static displacement of a system = F/K_{tot}
Y^D	=	open circuit electrical admittance of the piezoelectric (inherent capacitance)
Y^{EL}	=	electrical admittance of the piezoelectric (sum of shunting admittance in parallel to the inherent capacitance)
Y^{SU}	=	shunting admittance of the piezoelectric (in parallel to inherent capacitance)
Z	=	generic impedance, mechanical or electrical
Z^{ME}	=	effective mechanical impedance of the shunted piezoelectric
Z^{EL}	=	electrical impedance of the piezoelectric (shunting impedance in parallel to the inherent capacitance)
β	=	mass ratio (proof mass/system mass)
γ	=	complex nondimensional frequency = s/ω_n
δ	=	resonant shunted piezoelectric frequency tuning parameter, ω_e/ω_n
η	=	loss factor
ρ	=	nondimensional resistance (or frequency) = $RC^S_p\omega$
ω_e	=	resonant shunted piezoelectric electrical resonant frequency
ω_n	=	natural frequency of a 1-DOF system

Subscript

p	=	piezoelectric
PP	=	optimal by pole placement criteria
t	=	transpose of a vector or matrix
TF	=	optimal by transfer function criteria

Superscript

E	=	value taken at constant field (short circuit)
D	=	value taken at constant electrical displacement (open circuit)
RES	=	pertaining to resister shunting
RSP	=	pertaining to resonant circuit shunting
S	=	value taken at constant strain (clamped)
SU	=	shunted value
T	=	value taken at constant stress (free)

Introduction

There are many applications where the addition of passive vibration damping to a structural system can greatly increase the systems performance or stability. The addition of passive damping can decrease peak vibration amplitudes in structural systems and add robustness to marginally stable active control systems, Ref [1]. Structural damping can be increased by several methods the most common being the addition of high loss factor viscoelastic materials to the structure or the attachment of a mechanical vibration absorber.

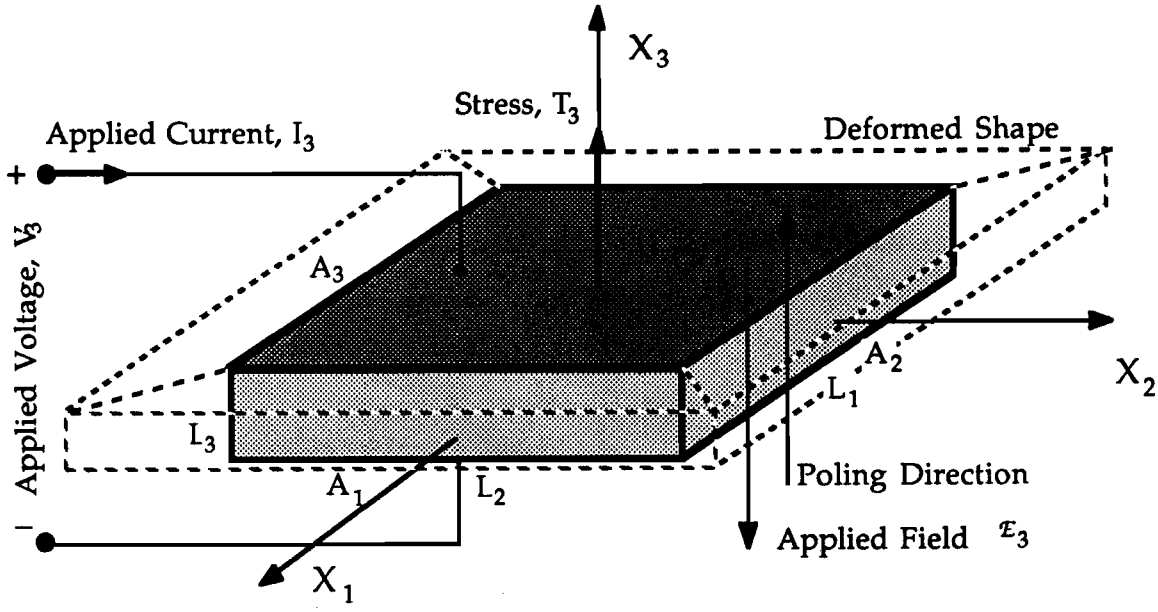

Figure 1: Assumed Geometry for a Typical Piezoelectric Material with the Top and Bottom Surfaces Electroded

In recent years piezoelectric elements have been used as embedded sensors and actuators in smart structures by Crawley and deLuis [2] and Hagood [3] and as elements of active vibration suppression system for cantilevered beams by Hanagud [4] and Hubbard [5]. They have also been used as actuation components in wave control experiments by Pines and von Flotow [6]. Within active control systems, the piezoelectrics require complex amplifiers and associated sensing electronics. These can be eliminated in passive shunting applications where the only external element is a simple passive electrical circuit. The shunted piezoelectric itself can also be used as a structural actuator in a control system.

This paper presents a new type of passive damping mechanism for structural systems which uses piezoelectric materials bonded to the structure. Piezoelectric materials possess certain properties which make them useful as dampers or control elements for structures. The first is that they strain when an electrical field is applied across them. This property makes them well suited as actuators for control systems (where the control signal is typically an applied voltage. The second is that they produce a voltage under strain. This property makes them well suited for sensing strain. In general, piezoelectrics have the ability to efficiently transform mechanical energy to electrical energy and vice-versa. It is this transformation ability which makes them useful as structural dampers.

The advantages to this type of passive piezoelectric application were first presented by Forward [7] & [8] and Edwards and Miyakawa [9] for damping applications on resonant structures. This paper establishes the derivation and analytical foundation for analysis of general systems with shunted piezoelectrics. A typical piezoelectric element is shown in Fig. (1). The fundamental constitutive relations are the relation between strain and applied field, known as the d constants, and between the charge density and the applied strain known as the g constants. Another fundamental property is the electromechanical coupling coefficient, k, which governs the energy transformation properties of a piezoelectric. The constants are explained in detail in Ref. [10].

In passive energy dissipation applications, the electrodes of the piezoelectric are shunted with some electrical impedance; hence the term shunted piezoelectrics is used. The electrical impedance is designed to dissipate the electrical energy which has been converted from mechanical energy by the piezoelectric. In the following sections, the shunted

piezoelectric's interaction with external circuits will be modeled, and the benefits that can be derived by passive circuit shunting of piezoelectrics will be quantified. First, the equivalent effective impedance of the shunted piezoelectric will be derived. This expression will then be applied to the cases of resistive and resonant circuit shunting. Expressions for the system damping will be derived, and parameters will be found which maximize this damping. An experiment verifies the accuracy of the analysis.

Modelling of Generally Shunted Piezoelectric Materials

A general expression for the material constants of a linear piezoelectric can be written from Ref. [11] as:

$$\begin{bmatrix} \boldsymbol{D} \\ \boldsymbol{S} \end{bmatrix} = \begin{bmatrix} \boldsymbol{\varepsilon}^{T} & \boldsymbol{d} \\ \boldsymbol{d}_{t} & \boldsymbol{s}^{E} \end{bmatrix} \begin{bmatrix} \boldsymbol{E} \\ \boldsymbol{T} \end{bmatrix} \tag{1}$$

where **D** is a vector of electrical displacements (charge/area), **E** is the vector of electrical field applied to the material (volts/meter), **S** is the vector of material strains, and **T** is the vector of material stresses (force/area).

$$\boldsymbol{D} = \begin{bmatrix} D_1 \\ D_2 \\ D_3 \end{bmatrix}, \quad \boldsymbol{E} = \begin{bmatrix} E_1 \\ E_2 \\ E_3 \end{bmatrix}, \quad \boldsymbol{S} = \begin{bmatrix} S_{11} \\ S_{22} \\ S_{33} \\ S_{23} \\ S_{13} \\ S_{12} \end{bmatrix} = \begin{bmatrix} S_1 \\ S_2 \\ S_3 \\ S_4 \\ S_5 \\ S_6 \end{bmatrix}, \quad \boldsymbol{T} = \begin{bmatrix} T_{11} \\ T_{22} \\ T_{33} \\ T_{23} \\ T_{13} \\ T_{12} \end{bmatrix} = \begin{bmatrix} T_1 \\ T_2 \\ T_3 \\ T_4 \\ T_5 \\ T_6 \end{bmatrix} \tag{2}$$

The 3 direction is associated with the direction of poling and the material is approximately isotropic in the other two directions. These direction conventions are shown in Fig. (1). The matrix which relates the two electrical variables, electrical displacement and electrical field, contains the dielectric constants for the material. This matrix can be written:

$$\boldsymbol{\varepsilon}^{T} = \begin{bmatrix} \varepsilon_1^{T} & 0 & 0 \\ 0 & \varepsilon_1^{T} & 0 \\ 0 & 0 & \varepsilon_3^{T} \end{bmatrix} \tag{3}$$

where the superscript, $()^{T}$, signifies that the values are measured at constant stress. The two elastic variables, stress and strain, are related through the compliance matrix of the piezoceramic, which has the form:

$$\boldsymbol{s}^{E} = \begin{bmatrix} s_{11}^{E} & s_{12}^{E} & s_{13}^{E} & 0 & 0 & 0 \\ s_{12}^{E} & s_{11}^{E} & s_{13}^{E} & 0 & 0 & 0 \\ s_{13}^{E} & s_{13}^{E} & s_{33}^{E} & 0 & 0 & 0 \\ 0 & 0 & 0 & s_{55}^{E} & 0 & 0 \\ 0 & 0 & 0 & 0 & s_{55}^{E} & 0 \\ 0 & 0 & 0 & 0 & 0 & s_{66}^{E} \end{bmatrix} \tag{4}$$

where the superscript, $()^E$, signifies that the values are measured at constant electrical field (eg. short circuit). Note that due to symmetry the material properties are identical in the 1 and 2 directions.

Finally, there are those terms which couple the mechanical and electrical equations by virtue of the piezoelectric effect. In the form of the equations given in (1) the coupling terms are the piezoelectric constants which relate strain to applied field. For piezoelectric ceramics, the matrix of piezoelectric constants has the form:

$$\boldsymbol{d} = \begin{bmatrix} 0 & 0 & 0 & 0 & d_{15} & 0 \\ 0 & 0 & 0 & d_{15} & 0 & 0 \\ d_{31} & d_{31} & d_{33} & 0 & 0 & 0 \end{bmatrix} \tag{5}$$

The first term in the subscript refers to the electrical axis while the second refers to the mechanical. Thus d_{31} refers to the strain developed in the 1 direction in response to a field in the 3 direction (parallel to the material poling).

In order to allow the use of traditional concepts of electrical admittance and impedance for the shunting analysis it is necessary to perform a change of variables. If we use the definitions for voltage and current in Ref. [10]:

$$V_i = \int_0^{L_i} \boldsymbol{E} \cdot d\,\boldsymbol{x}_i \tag{6a}$$

$$I_i = \int_{A_i} \dot{\boldsymbol{D}} \cdot d\,\boldsymbol{a}_i \tag{6b}$$

and furthermore assume that the field within and electrical displacement on the surface are uniform for the piezoelectric material, then linear relationships can be defined in the Laplace domain:

$$\begin{aligned} \boldsymbol{V}(s) &= \boldsymbol{L} \cdot \boldsymbol{E}(s), \\ \boldsymbol{I}(s) &= s\boldsymbol{A} \cdot \boldsymbol{D}(s) \end{aligned} \tag{7a &b}$$

where **L** is a diagonal matrix of the lengths of the piezoelectric bar in the i^{th} direction, **A** is the diagonal matrix of the areas of surfaces perpendicular to the i^{th} direction, and s is the Laplace parameter.

Taking the Laplace transform of eq. (1) and using eqs. (7a&b) to eliminate **E** and **D**, the general equation for a piezoelectric in terms of the external current input and applied voltage is obtained.

$$\begin{bmatrix} \boldsymbol{I} \\ \boldsymbol{S} \end{bmatrix} = \begin{bmatrix} s\boldsymbol{A}\,\varepsilon^T\,\boldsymbol{L}^{-1} & s\boldsymbol{A}\boldsymbol{d} \\ \boldsymbol{d}_t\boldsymbol{L}^{-1} & \boldsymbol{s}^E \end{bmatrix} \begin{bmatrix} \boldsymbol{V} \\ \boldsymbol{T} \end{bmatrix} \tag{8}$$

This equation can be further simplified by noting that the upper left partition of the generalized compliance matrix is diagonal. The elements of this partition have the form:

$$\frac{A_i \varepsilon_i^T}{L_i} = C_{pi}^T \tag{9}$$

where C_{pi} is the capacitance between the surfaces perpendicular to the i^{th} direction. Noting that sC_p is the open circuit admittance of the piezoelectric material, eq. (8) can thus be written:

$$\begin{bmatrix} I \\ S \end{bmatrix} = \begin{bmatrix} sC_p^T & sAd \\ d_t L^{-1} & s^E \end{bmatrix} \begin{bmatrix} V \\ T \end{bmatrix} = \begin{bmatrix} Y^D(s) & sAd \\ d_t L^{-1} & s^E \end{bmatrix} \begin{bmatrix} V \\ T \end{bmatrix} \tag{10}$$

where $\mathbf{Y}^D(s)$ is the open circuit admittance of the piezoelectric (the inherent capacitance with free mechanical boundary conditions). The open circuit admittance relates the voltage applied across the piezoelectric's electrodes in Fig. (2) to the external current input into the piezoelectric . The large leakage resistance of the piezoelectric material is treated as infinite in this analysis but can easily be included as a modifying term.

For shunted piezoelectric applications, a passive electrical circuit is connected between the surface electrodes as shown in one dimension in Fig. (2). Since the circuit is placed across the electrodes, it appears in parallel to the inherent piezoelectric capacitance in that direction. Since admittances in parallel add, the governing constitutive equations for a shunted piezoelectric material become:

$$\begin{bmatrix} I \\ S \end{bmatrix} = \begin{bmatrix} Y^{EL} & sAd \\ d_t L^{-1} & s^E \end{bmatrix} \begin{bmatrix} V \\ T \end{bmatrix} \tag{11}$$

with:

$$Y^{EL} = Y^D + Y^{SU} \tag{12}$$

The externally applied current, **I**, is the sum of the currents flowing through the shunting impedance, the inherent piezoelectric capacitance, and the piezoelectric transformer. The shunting admittance matrix is assumed diagonal and frequency dependant with the form:

$$Y^{SU} = \begin{bmatrix} Y_1^{SU} & 0 & 0 \\ 0 & Y_2^{SU} & 0 \\ 0 & 0 & Y_3^{SU} \end{bmatrix} \tag{13}$$

The top partition of eq. (11) can be solved for the voltage appearing across the electrodes.

$$V = Z^{EL} I - Z^{EL} sAdT \tag{14}$$

Where $\mathbf{Z}^{EL}$ is the electrical impedance matrix and is equal to $(\mathbf{Y}^{EL})^{-1}$. The electrical impedance matrix is also diagonal. Equation (14) can be substituted into (11) to find an expression for the strain in terms of stress and input current.

$$S = \left[s^E - d_t L^{-1} Z^{EL} sAd\right] T + \left[d_t L^{-1} Z^{EL}\right] I \tag{15}$$

This is a governing equation for a shunted piezoelectric. It gives the strain for a given applied stress and forcing current. Notice that shunting the piezoelectric does not preclude use of the shunted element as an actuator in an active control system but rather modifies the passive characteristics of the actuator. By modifying the passive stiffness of

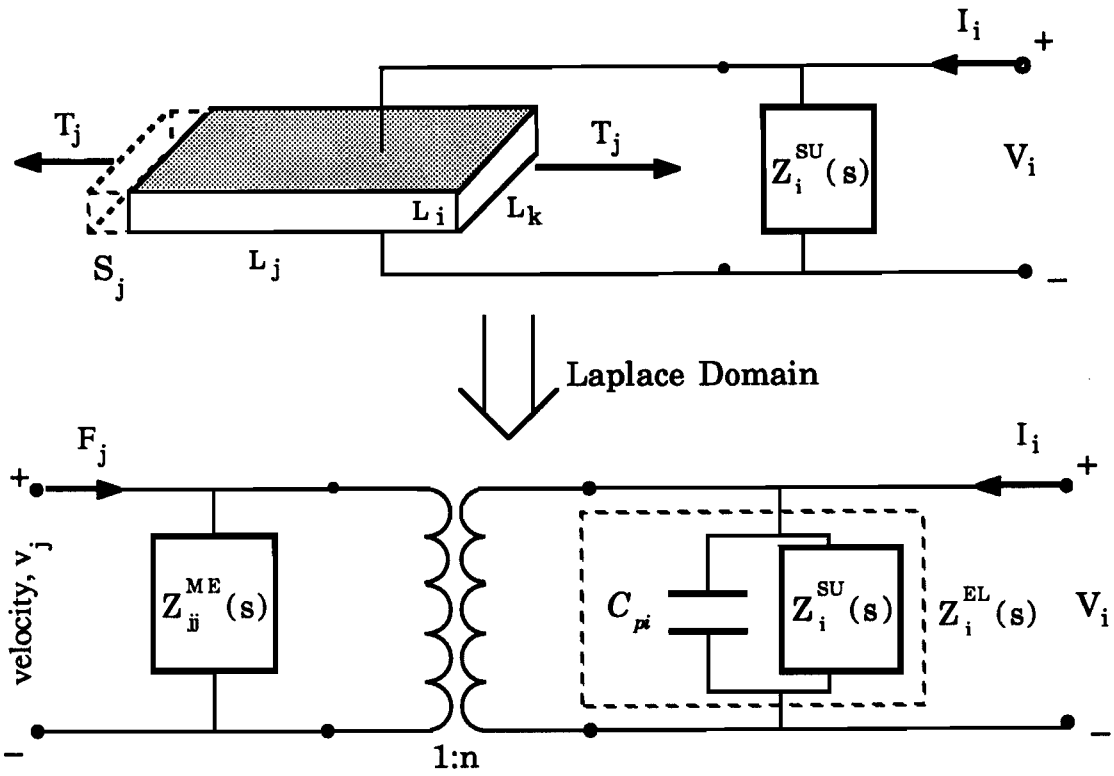

Figure 2: Simple Physical Model of a Shunted Piezoelectric and its Network Analog Showing its Ability to Transform Energy from Mechanical to Electrical and Vice Versa.

the piezoelectric to include material damping, perfectly colocated damping can be introduced into the system. This passive damping can be useful in stabilizing controlled structures in the manner of Ref. [12] in which a mechanical actuator is passively damped.

Of particular importance is the new mechanical compliance term. The shunted piezoelectric compliance can be defined from (15):

$$\boldsymbol{s}^{SU} = \left[\boldsymbol{s}^{E} - \boldsymbol{d}_t \boldsymbol{L}^{-1} \boldsymbol{Z}^{EL} s \boldsymbol{A} \boldsymbol{d}\right] \tag{16}$$

If we note that with constant stress:

$$\boldsymbol{Z}^{E}(s) = \boldsymbol{0} = \text{short circuit electrical impedance} \tag{17a}$$

$$\boldsymbol{Z}^{D}(s) = (\boldsymbol{C}_p^{T} s)^{-1} = \text{open circuit electrical impedance} \tag{17b}$$

and that:

$$s \boldsymbol{L}^{-1} \varepsilon^{T} \boldsymbol{A} = \boldsymbol{C}_p^{T} s \tag{18}$$

equation (16) can be put in the form

$$\boldsymbol{s}^{SU} = \left[\boldsymbol{s}^{E} - \boldsymbol{d}_t \bar{\boldsymbol{Z}}^{EL} (\varepsilon^{T})^{-1} \boldsymbol{d}\right] \tag{19}$$

where the matrix of nondimensional electrical impedances is defined:

$$\bar{\mathbf{Z}}^{EL} = \mathbf{Z}^{EL}(\mathbf{Z}^{D})^{-1} \tag{20}$$

Finally, since $\mathbf{Z}^{EL}$ is diagonal, the electrical contribution to the compliance can simply be written as a summation over the electrical impedances:

$$\mathbf{s}^{SU} = \left[\mathbf{s}^{E} - \sum_{i=1}^{3}\left[\bar{Z}_i^{EL}\left(\frac{1}{\varepsilon_i^{T}}\mathbf{d}_i\mathbf{d}_i\right)\right]\right] = \left[\mathbf{s}^{E} - \sum_{i=1}^{3}\bar{Z}_i^{EL}\mathbf{M}_i\right] \tag{21}$$

where $\mathbf{d}_i$ denotes the i^{th} row of $\mathbf{d}$ and for piezoelectric ceramics the $\mathbf{M}_i$ have the form:

$$\mathbf{M}_1 = \frac{1}{\varepsilon_1^{T}}\begin{bmatrix} 0 & 0 & 0 & 0 & 0 & 0 \\ 0 & 0 & 0 & 0 & 0 & 0 \\ 0 & 0 & 0 & 0 & 0 & 0 \\ 0 & 0 & 0 & 0 & 0 & 0 \\ 0 & 0 & 0 & 0 & d_{15}^2 & 0 \\ 0 & 0 & 0 & 0 & 0 & 0 \end{bmatrix} \quad \mathbf{M}_2 = \frac{1}{\varepsilon_1^{T}}\begin{bmatrix} 0 & 0 & 0 & 0 & 0 & 0 \\ 0 & 0 & 0 & 0 & 0 & 0 \\ 0 & 0 & 0 & 0 & 0 & 0 \\ 0 & 0 & 0 & d_{15}^2 & 0 & 0 \\ 0 & 0 & 0 & 0 & 0 & 0 \\ 0 & 0 & 0 & 0 & 0 & 0 \end{bmatrix} \tag{22a\&b}$$

$$\mathbf{M}_3 = \frac{1}{\varepsilon_3^{T}}\begin{bmatrix} d_{31}^2 & d_{31}^2 & d_{31}d_{33} & 0 & 0 & 0 \\ d_{31}^2 & d_{31}^2 & d_{31}d_{33} & 0 & 0 & 0 \\ d_{31}d_{33} & d_{31}d_{33} & d_{33}^2 & 0 & 0 & 0 \\ 0 & 0 & 0 & 0 & 0 & 0 \\ 0 & 0 & 0 & 0 & 0 & 0 \\ 0 & 0 & 0 & 0 & 0 & 0 \end{bmatrix} \tag{22c}$$

These equations constitute a general expression for the compliance matrix of a piezoelectric element with arbitrary electrode placement or elastic boundary conditions. Several things are apparent from eq. (21). First, electroding and shunting the piezoelectric element in the directions perpendicular to the poling direction (3) of the piezoelectric can only effect the shear terms of the compliance. Secondly, shunting the piezoelectric in the 3 direction modifies all of the non-shear terms of the compliance matrix. Finally, the electrical shunting circuit's ability to modify the piezoelectric material properties depends on both the material piezoelectric constants and the nondimensional electrical impedance.

Specialization to Uniaxial Loading Cases

Equation (21) simplifies greatly when the piezoelectric element is loaded uniaxially with either a normal or shear stress and only one pair of electrodes are present providing an external electric field with components in only one direction. These common modes of operation can be described:

Longitudinal Case: Force and field in the 3 direction

Transverse Case: Force in 1 or 2 direction; Field in 3 direction

Shear Case: Force in 4 or 5 direction (shear); Field in 2 or 1 direction respectively

With uniaxial loading in the j^{th} direction, only a single term from the compliance matrix contributes to the material strain energy. By examining that term the energy dissipation properties of the shunted piezoelectric can be examined. For loading in the j^{th} direction and the field in the i^{th} direction the term in the compliance matrix is:

$$s_{jj}^{SU} = s_{jj}^{E} - \bar{Z}_i^{EL}(M_i)_{jj} = s_{jj}^{E} - \bar{Z}_i^{EL}\frac{(d_{ij})^2}{\varepsilon_i^T} \tag{23}$$

where the subscripts denote the row and column of the respective matrix.

At this point it is convenient to introduce the piezoelectric property known as the electromechanical coupling coefficient. It is defined as the ratio of the peak energy stored in the capacitor to the peak energy stored in the material strain (under uniaxial loading and sinusoidal motion) with the piezoelectric electrodes open. Physically, its square represents the percentage of mechanical strain energy which is converted into electrical energy and vice-versa. For the 3 cases of piezoelectric operation considered, the electromechanical coupling coefficients are defined in Ref. [10]:

$$\text{Shear:}\quad k_{15} = \frac{d_{15}}{\sqrt{s_{55}^E \varepsilon_1^T}} = k_{24}$$

$$\text{Transverse:}\quad k_{31} = \frac{d_{31}}{\sqrt{s_{11}^E \varepsilon_3^T}} = k_{32}$$

$$\text{Longitudinal:}\quad k_{33} = \frac{d_{33}}{\sqrt{s_{33}^E \varepsilon_3^T}} \tag{24}$$

or in the notation used before for force in the j^{th} direction and field in the i^{th} direction:

$$k_{ij} = \frac{d_{ij}}{\sqrt{s_{jj}^E \varepsilon_i^T}} \tag{25}$$

Substituting eq. (25) into (23) we obtain:

$$s_{jj}^{SU} = s_{jj}^{E}\left[1 - k_{ij}^2 \bar{Z}_i^{EL}\right] \tag{26}$$

From eq. (26) we can see that the compliance of the shunted piezoelectric is related to the short circuit compliance of the piezoelectric material modified by a nondimensional term which depends on the electrical shunting circuit and the material's electromechanical coupling coefficient. From eq. (26) the relation between the short circuit and open circuit compliance of the piezoelectric can be derived by noting that in the open circuit case

$$\bar{Z}^{EL} = 1 \tag{27}$$

and thus eq. (26) reduces to:

$$s_{jj}^{D} = s_{jj}^{E}\left[1 - k_{ij}^2\right] \tag{28}$$

which is in agreement with the relation given in Ref. [10] for the cases considered.

Equation (28) gives the change in mechanical properties of the piezoceramic as the electrical boundary conditions are changed (from short circuit to open circuit). An analogous relation can be derived for the change in the piezoelectric inherent capacitance as the mechanical boundary conditions are changed. For uniaxial field and loading (only the boundary conditions in the loading direction are varied) this relation is also dependant on the electromechanical coupling coefficient.

$$C_{pi}^{S} = C_{pi}^{T}\left[1 - k_{ij}^{2}\right] \tag{29}$$

This equation will be used for nondimensionalizations in the coming sections.

Equation (28) can be used with (26) to derive a nondimensional expression for the mechanical impedance of the shunted piezoelectric. For uniaxial loading in the j^{th} direction, the mechanical impedance of the piezoelectric can be expressed as a function of the Laplace parameter, s, as:

$$Z_{jj}^{ME}(s) = \frac{A_j}{s_{jj} L_j s} \tag{30}$$

Now using eq. (30) and (26) to define the impedance of the shunted piezoelectric and eq. (28) to nondimensionalize, the final expression for the nondimensionalized mechanical impedance of the shunted piezoelectric can be derived:

$$\bar{Z}_{jj}^{ME}(s) = \frac{Z_{jj}^{SU}}{Z_{jj}^{D}} = \frac{1 - k_{ij}^{2}}{1 - k_{ij}^{2}\,\bar{Z}_{i}^{EL}(s)} \tag{31}$$

where the functional dependance of the mechanical and electrical impedances is written explicitly; and the nondimensional mechanical impedance is defined as the ratio of the shunted mechanical impedance to the open circuit impedance.

Coupling Shunted Piezoelectrics to Structures

The nondimensional mechanical impedance, $\bar{Z}^{ME}$, can be complex and frequency dependant since it depends on the complex, frequency dependant electrical impedance. If we note that the impedance is primarily a stiffness, then we can represent the impedance as a complex modulus, as is typically done in material damping. This is especially useful if the shunting impedance is not resonant.

$$\bar{Z}_{jj}^{ME}(s) = \bar{E}_{jj}(\omega)\left[1 + i\eta_{jj}(\omega)\right] \tag{32}$$

where $\bar{E}$ is the ratio of shunted stiffness to open circuit stiffness of the piezoelectric and η is the material loss factor. This reduction leads to frequency-dependent equations for the complex modulus of the shunted piezoelectric. Comparing eq. (32) to eq. (31) gives the frequency dependant equivalent material properties for an arbitrarily shunted piezoelectric.

Loss Factor:
$$\eta(\omega) = \frac{\mathrm{Im}\left\{\bar{Z}^{ME}(s)\right\}}{\mathrm{Re}\left\{\bar{Z}^{ME}(s)\right\}} \tag{33a}$$

Modulus: $$\bar{E}(\omega) = \mathrm{Re}\left\{\bar{Z}^{ME}(s)\right\} \tag{33b}$$

These equations, as well as (31), can be applied to arbitrary shunting conditions for parameter optimization of the material loss factor at a critical frequency.

To find the total system loss factor, the expression for the effective impedance of the shunted piezoelectric, eq. (31) can be used along with the impedances of the other damping devices in the frequency domain system analysis described in Ref. [13]. In general, just as for viscoelastic materials, the relation between the high loss factor of a structural component and the loss factor of the total structure can be represented as an average of the system component loss factors weighted by the fraction of strain energy in the respective elements, Ref. [14]

$$\eta^{TOT} = \frac{\sum_{i=1}^{n} \eta_i U_i}{\sum_{i=1}^{n} U_i} \tag{34}$$

where U_i is the peak strain energy in the i^{th} element of the structure. Techniques for improving structural damping typically employ the damping material (shunted piezoelectrics or viscoelastics) in areas of high strain energy to take advantage of this weighting. The stiffness and loss factor of damping materials are typically frequency dependant. The high stiffness (63 GPa) of the shunted piezoelectric gives them advantages over viscoelastic materials (circa 1 MPa) since for a given strain they can store many times the strain energy of the viscoelastic and thus contribute to higher system loss factors. The piezoelectric material properties are also relatively temperature independent below their Curie temperature (temperature at which they lose their piezoelectric properties) Ref. [11]. For commonly available piezoelectrics this is typically in the range of several hundred °C.

Application: Resistive Shunting

A resistor can shunt the piezoelectric electrodes as shown in Fig. (3). In this shunting geometry, the resistor is placed in parallel with the inherent capacitance of the piezoelectric. The resistor provides a means of energy dissipation on the electrical side and thus should increase the total piezoelectric loss factor above the loss factor for the short or open circuited piezoelectric. Its exact effect on the stiffness and dissipation properties of the piezoelectric can be modelled by applying eq. (31). For the case of a resistor across the piezoelectric electrodes, the total nondimensional electrical impedance in the i^{th} direction is:

$$Z_i^{SU}(s) = R_i \tag{35a}$$

$$\bar{Z}_i^{EL}(s) = \frac{Z_i^{EL}(s)}{Z_i^{D}(s)} = \frac{R_i C_{pi}^{T} s}{R_i C_{pi}^{T} s + 1} \tag{35b}$$

Eq. (35b) can be substituted into Eq. (31) to give an expression for the nondimensional mechanical impedance of a resistive shunted piezoelectric.

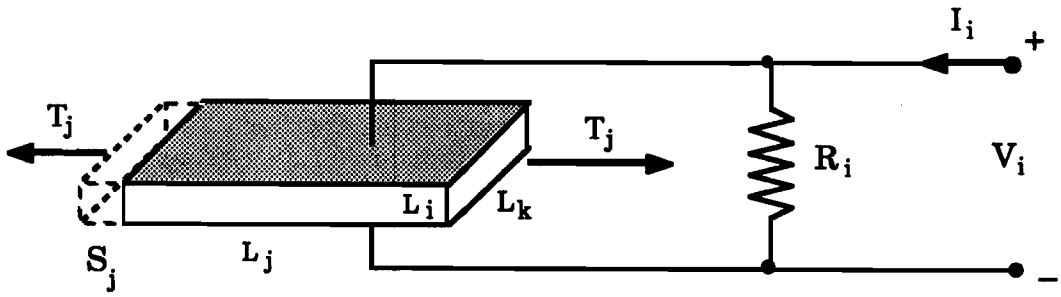

Figure 3: Resister Shunted Piezoelectric Schematic

$$\bar{Z}_{jj}^{RES}(s) = 1 - \frac{k_{kj}^2}{1 + i\rho_k} \tag{36a}$$

where ρ_k is the nondimensional frequency,

$$\rho_k = R_k C_{pk}^S \omega = \frac{\omega}{\omega_d} \tag{36b}$$

and C_{pi}^S was defined in eq. (29).

Materials Perspective

Since there are no internal resonances, it is convenient to use (33a & b) to express (36a) as a frequency dependent material stiffness and loss factor. The resistor can be thought of as changing the material properties of the piezoelectric into those of a lossy material similar to a viscoelastic in behavior. Using (33a & b) to solve for nondimensionalized expressions for η and E gives:

$$\eta_{jj}^{RES}(\omega) = \frac{\rho_i k_{ij}^2}{(1 - k_{ij}^2) + \rho_i^2} \tag{37a}$$

$$\bar{E}_{jj}^{RES}(\omega) = 1 - \frac{k_{ij}^2}{1 + \rho_i^2} \tag{37b}$$

These relations have been plotted versus ρ, the nondimensional frequency (or the nondimensional resistance) in Fig. (4) for typical values of the longitudinal and transverse coupling coefficients. These curves are similar to the equivalent material curves for a standard linear solid. As illustrated in the graphs, for a given resistance the stiffness of the piezoelectric changes from its short-circuit value at low frequencies to its open-circuit value at high frequencies. The frequency of this transition is determined by the shunting resistance. The material also exhibits a maximum loss factor at this transition point. The value of this maximum loss factor can be found to be:

$$\eta_{max-jj}^{RES} = \frac{k_{ij}^2}{2 \cdot \sqrt{1 - k_{ij}^2}} \tag{38a}$$

at a nondimensional frequency of:

$$\rho_i = R_i C_{pi}^S \omega = \sqrt{1 - k_{ij}^2} \tag{38b}$$

Thus by appropriate choice of resistor, the peak of the loss factor curve can be moved to the desired frequency.

It is worthwhile to draw a comparison between resistively shunted piezoelectrics and viscoelastic materials. The form of the frequency dependence of the viscoelastic can be seen in Ref. [14] for typical damping materials. For common viscoelastic materials, the peak loss factor occurs in a narrow frequency and temperature range where the viscoelastic is in transition from its rubbery state to its glassy state. This placement is directly analogous to the peak loss factor of the piezoelectric occurring at the transition from short circuit to open circuit stiffness.

It should be noted that the loss factor curve takes the same form as the standard relaxation curve for material damping, but can lead to material loss factors as high as 8.2% in the transverse case and 42.5% in the longitudinal or shear cases for commonly available piezoelectric ceramic materials. This compares favorably to the results obtained in Ref. [9] for the effective material loss factor for a resistive shunted piezoelectric ceramic.

While these loss factor levels are not as high as those for viscoelastics, the piezoelectric material (typically a ceramic) has higher stiffness than most viscoelastic materials and thus stores more strain energy for a given strain. The piezoelectric ceramic material properties also have the advantage of being relatively stable with temperature over their operating range. Since their main constituant is lead, however, their density is 8 times that of water. In all, the net effect is that in most structural cases shunted piezoelectrics will provide higher total structural damping levels per unit mass with higher temperature stability. These results for the resistive shunted piezoelectrics have been validated experimentally and will be presented in a later section.

Systems Perspective for Determining Resistive Shunted Piezoelectric Effectiveness

Since the stiffness of the piezoelectric material is frequency dependant, maximizing the loss factor of the piezoelectric material does not necessarily maximize the loss factor of the total structural system of which the piezoelectric is a part. As shown by eq. (34) the total damping of the system consists of the component damping weighted by the strain energy fraction in that component. This strain energy fraction is frequency dependant for shunted piezoelectrics since the piezoelectric stiffness varies with frequency. In order to accurately model the system modal damping as a function of frequency or shunting parameters (such as resistance), this frequency dependant stiffness must be carried through the calculations.

Another method of obtaining the system modal damping which yields significant insight into the problem is to represent a single mode of the system as a simple 1-DOF system with a piezoelectric component in parallel to the system stiffness as shown in Fig. (5). The mass and stiffness in the simple system can represent the modal mass and stiffness of a multi-DOF system. In this case the modal stiffness of the piezoelectric should also be used. The modal velocity of the piezoelectric system can be expressed in the Laplace domain as:

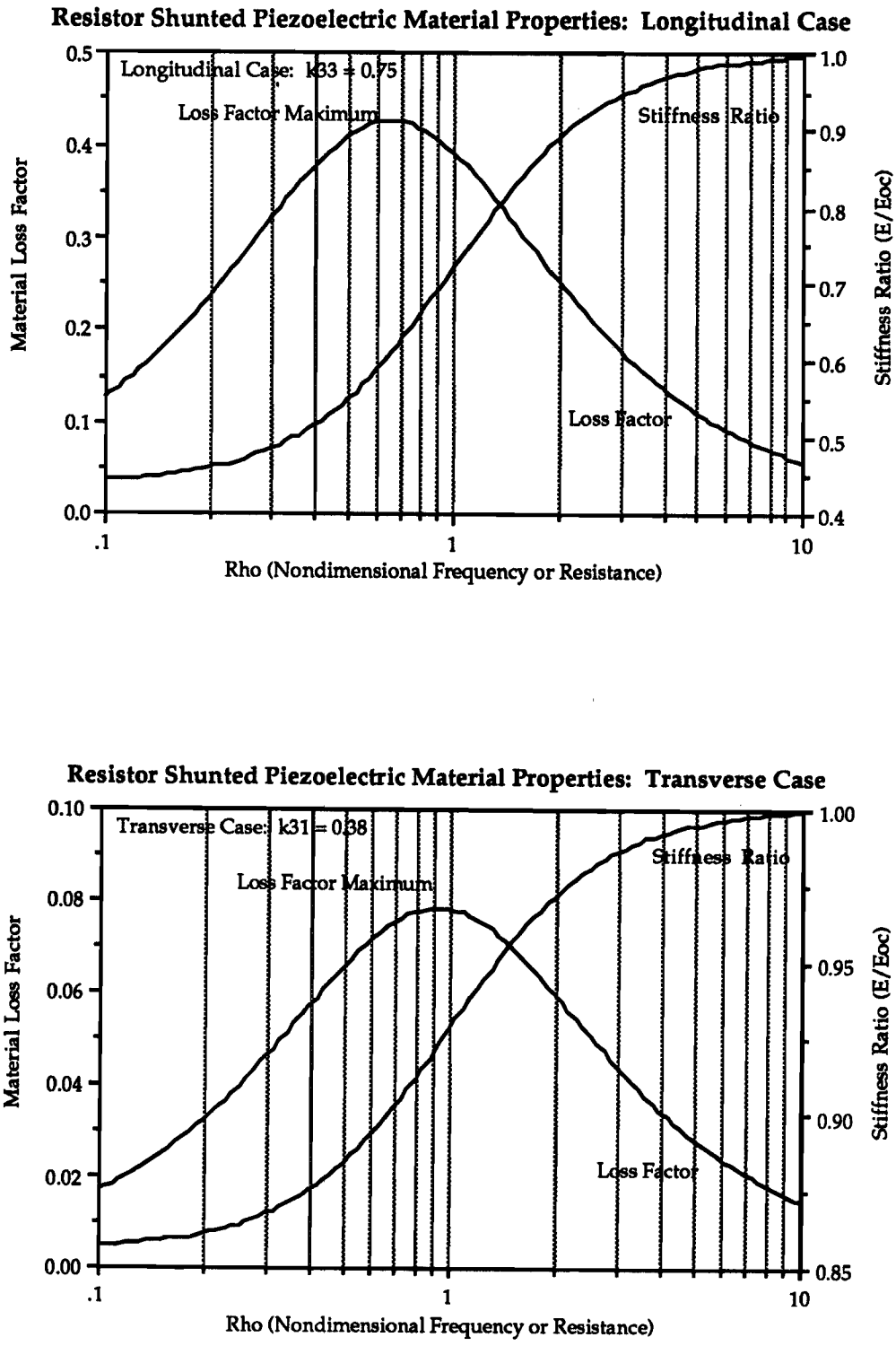

Figure 4: Effective Material Properties of a Resistively Shunted Piezoelectric in the Longitudinal (Upper) or Transverse (Lower) Cases

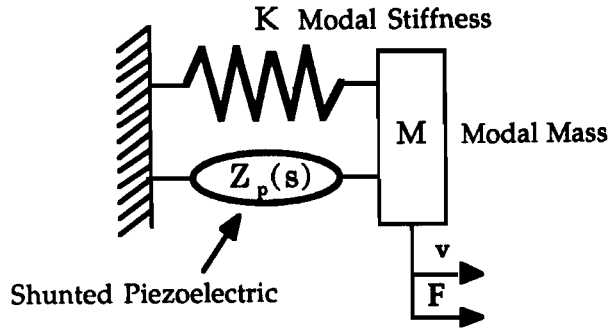

Figure 5: 1-DOF System with Shunted Piezoelectric Element in Parallel with the System Modal Mass

$$v(s) = \frac{F(s)}{Ms + \frac{K}{s} + Z_{jj}^{RES}(s)} \tag{39}$$

Where Ms is the impedance associated with the modal mass; K/s is the impedance associated with the modal stiffness; and $Z^{RES}(s)$ is the impedance associated with the resonant shunted piezoelectric's contribution to the modal mass. After reduction and nondimensionalization an expression for the position transfer function of such a mechanical system with a shunted piezoelectric in parallel with the base system stiffness and a force acting on the mass can be found from eq. (39):

$$\frac{x}{x^{ST}} = \frac{r\gamma + 1}{r\gamma^3 + \gamma^2 + r\left(1 + K_{ij}^2\right)\gamma + 1} \tag{40}$$

where x^{ST} is used for F/K_{tot} and K_{tot} is the sum of the base system modal stiffness and the piezoelectric open circuit modal stiffness. The nondimensionalization is defined relative to the mechanical system's natural frequency with the piezoelectric open circuited.

$$\omega_n^E = \sqrt{\frac{K + K_{jj}^E}{M}} \tag{41a}$$

$$\gamma = \frac{s}{\omega_n^E} = \text{nondimensional frequency} \tag{41b}$$

$$r = R_i C_{pi}^S \omega_n^E = \rho\big|_{\omega = \omega_n^E} = \text{electrical damping ratio} \tag{41c}$$

The generalized electromechanical coupling coefficient, K_{ij}, is defined:

$$K_{ij}^2 = \left(\frac{K_{jj}^E}{K + K_{jj}^E}\right)\left(\frac{k_{ij}^2}{1 - k_{ij}^2}\right) = \bar{K}\frac{k_{ij}^2}{1 - k_{ij}^2} \tag{42}$$

where $\bar{K}$ is the ratio of piezoelectric short circuit modal stiffness to the total system modal stiffness. The generalized coupling coefficient reflects the fact that the piezoelectric is in parallel with some other stiffness, and thus a smaller fraction of the system strain energy is converted to electrical energy. It is proportional to the fraction of the system modal strain energy which is converted into electrical energy by the open circuit piezoelectric. As such, it is a direct measurement of a shunted piezoelectric's influence on a system.

The modal damping ratio can now be found exactly by solving for the roots of the cubic equation in the denominator of eq. (40), or approximately using commonly available root solvers. The exact technique was used to calculate the modal damping of the cantilevered beam test article.

Application: Resonant Circuit Shunting

Another case of interest is to create a resonant circuit by shunting the inherent capacitance of the piezoelectric with a resistor and inductor in series forming a LRC circuit for Z^{EL}. This circuit is shown in Fig. (6). This resonant electrical circuit can be tuned in the vicinity of a mode of the underlying mechanical system and thereby greatly increase the attainable modal damping ratio, in an effect similar to the classical proof-mass damper (PMD) or resonant vibration absorber.

With an inductor and a resistor in parallel with the piezoelectric's inherent capacitance, the total electrical impedance can be written:

$$Z_i^{SU}(s) = L_i s + R_i \tag{43a}$$

$$\bar{Z}_i^{EL}(s) = \frac{L_i C_{pi}^T s^2 + R_i C_{pi}^T s}{L_i C_{pi}^T s^2 + R_i C_{pi}^T s + 1} \tag{43b}$$

were L_i is the shunting inductance and R_i is the shunting resistance. This circuit is clearly resonant with some damping due to the resistance, R_i. Equation (43b) can be substituted into eq. (31) and the results nondimensionalized to obtain the nondimensional mechanical impedance of a resonant shunted piezoelectric:

$$\bar{Z}_{jj}^{RSP}(s) = 1 - k_{ij}^2 \left(\frac{\delta^2}{\gamma^2 + \delta^2 r \gamma + \delta^2} \right) \tag{44a}$$

where the nondimensionalizations are defined relative to some arbitrary normalization frequency, ω_n

$$\omega_e = \frac{1}{\sqrt{L_i C_{pi}^S}} = \text{electrical resonant frequency} \tag{44b}$$

$$\delta = \frac{\omega_e}{\omega_n} = \text{nondimensional tuning ratio} \tag{44c}$$

and γ and r are defined in eqs. (41b & c) respectively.

Equation (44) is an expression of the effective mechanical impedance of a piezoelectric element shunted by a resonant circuit. The key parameters of (44) are the

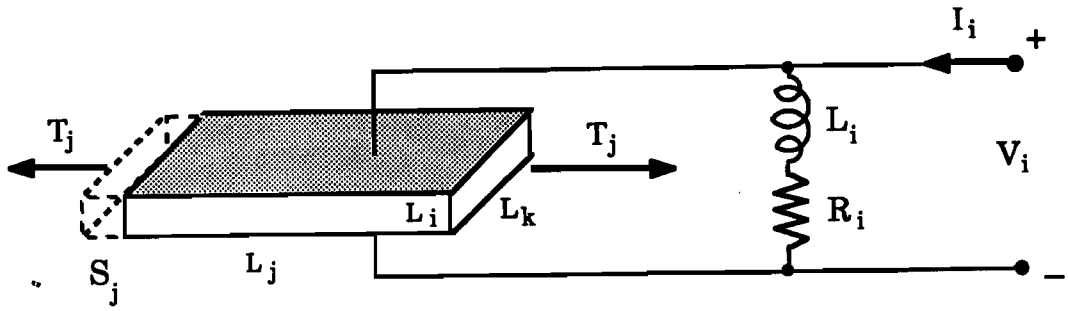

Figure 6: Resonant Shunted Piezoelectric Schematic

frequency tuning parameter, δ, and the damping parameter, r. These parameters are directly analogous to the ones used in classical proof mass damper nondimensionalization, Ref. [15]. The δ parameter reflects the frequency to which the electrical circuit is tuned, while the r parameter is an expression for the damping in the shunting circuit.

Materials Perspective

There are several ways to determine the parameters of eq. (44) which maximize energy dissipation. One of these involves treating the resonant shunted piezoelectric as a material with frequency dependant properties, in a fashion analogous to the resistive shunting case. The expression for the effective impedance of the piezoelectric can be put into a complex modulus form such as (33). This leads to complicated frequency-dependant expressions for the material stiffness and loss factor.

$$\bar{E}_{jj}^{RSP}(\omega) = 1 - k_{ij}^2\left(\frac{\delta^2(\delta^2 - g^2)}{(\delta^2 - g^2)^2 + (\delta^2 rg)^2}\right) \tag{45a}$$

$$\eta_{jj}^{RSP}(\omega) = \frac{k_{ij}^2\delta^2(\delta^2 rg)}{(\delta^2 - g^2)^2 + (\delta^2 rg)^2 - k_{ij}^2\delta^2(\delta^2 - g^2)} \tag{45b}$$

where E^{LRC} and η^{LRC} are the effective material properties of the resonant shunted piezoelectric, and g is the real form of γ, (ω/ω_n). These expressions can be seen plotted in Fig. (7) for common values of the parameters. They can be useful in system modelling if the values of the parameters are already known. Both the effective material stiffness and the damping vary nonlinearly with frequency and tuning parameter values, δ and r. This makes an optimization for energy dissipation difficult. The actual energy dissipated is dependant on both E and η and can be calculated for the total system using eq. (34).

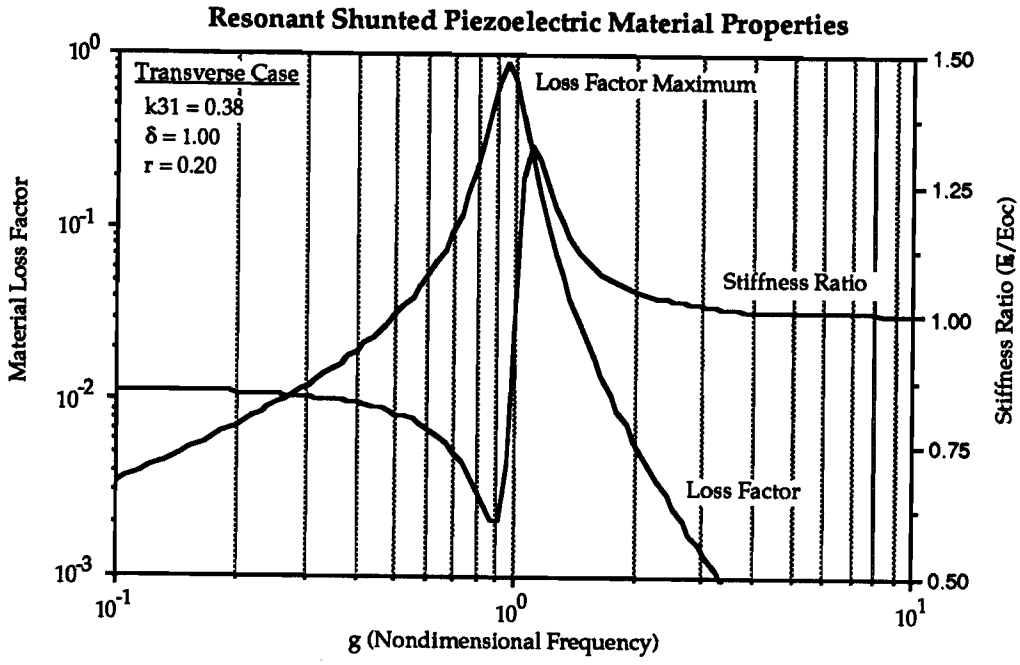

Figure 7: Effective Material Properties of a Piezoelectric Ceramic Operating Transversely and Shunted by a Resonant LRC Circuit.

Systems Perspective for Determining Resonant Shunted Piezoelectric's Effectiveness

The problems associated with the parameter optimization can be greatly alleviated by observing certain key similarities between a system containing a resonant shunted piezoelectrics (RSP) and a system containing a proof mass damper (PMD). As illustrated in Fig. (8), the similarities in system topologies suggest that the method for obtaining the optimum parameters for the PMD can be applied to the RSP. The derivation for optimal tuning and damping of the electrical circuit parallels the technique for determining the optimal tuning and damping ratio of a PMD as outlined in Ref. [15].

These two systems can be thought of as complementary since the proof mass damper appears as a point impedance in system modeling and thus damps out only the available kinetic energy. On the other hand, shunted piezoelectrics are modeled as multi-port impedances which derive their dissipation from the relative motion of two system nodes. Thus they can be thought of as dissipating structural strain energy. This difference will reflect on the optimum placement of the actual dampers.

Following the techniques of modeling the 1-DOF system presented in the section on resister shunting, the modal deformation rate of the piezoelectric system with resonant shunted piezoelectrics can be expressed in the Laplace domain as:

$$v(s) = \frac{F(s)}{Ms + \frac{K}{s} + Z_{ij}^{RSP}(s)} \tag{46}$$

Where Ms, K/s are modal quantities, and $Z^{RSP}(s)$ is the modal impedance associated with the resonant shunted piezoelectric. After reduction and nondimensionalization, an

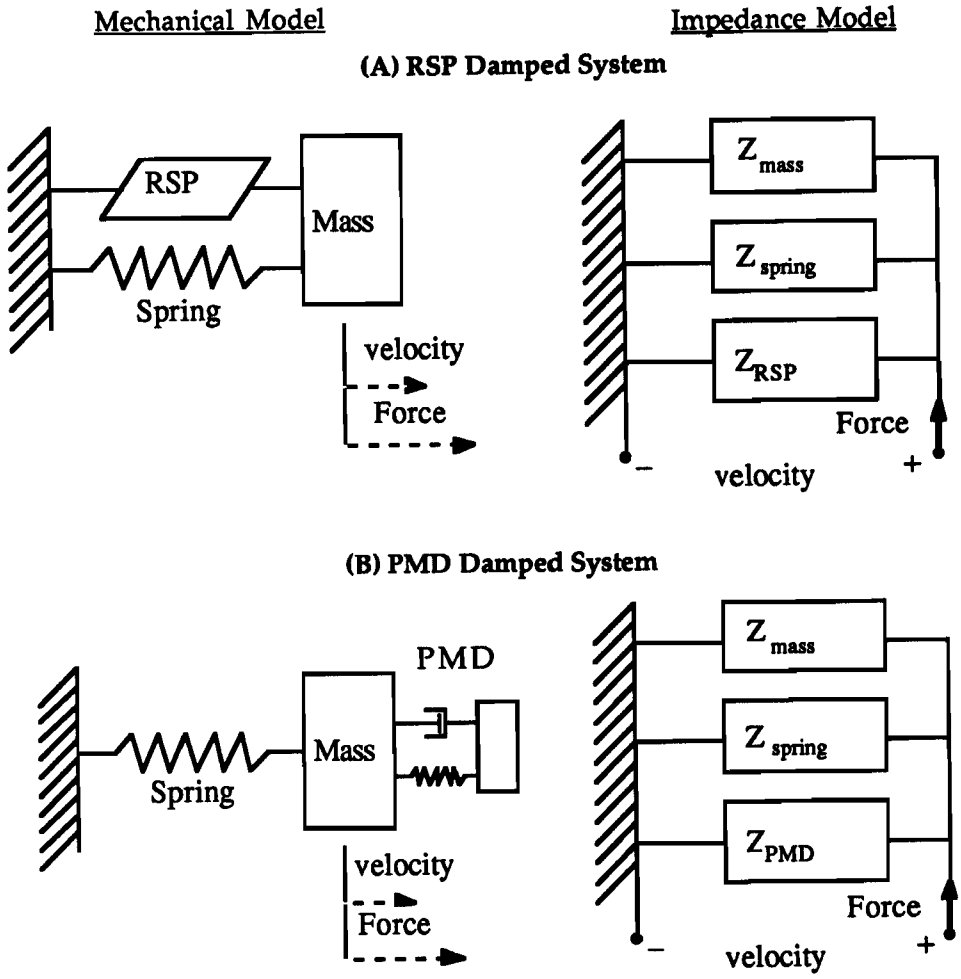

Figure 8: Comparison of Resonant Damper Topologies between an RSP Damped System (A) and a PMD Damped System (B)

expression for the position transfer function of a mechanical system with a RSP in parallel with the base system stiffness and a force acting on the mass can be found from (46):

$$\frac{x}{x^{ST}} = \frac{\left(\delta^2 + \gamma^2\right) + \delta^2 r\gamma}{\left(1+\gamma^2\right)\left(\delta^2 + \gamma^2 + \delta^2 r\gamma\right) + K_{ij}^2\left(\gamma^2 + \delta^2 r\gamma\right)} \tag{47}$$

where the nondimensionalization is the same as that used in eq. (44). The mechanical system's short circuit natural frequency (defined in eq. 41a) is substituted for the normalization frequency used in (44) and the generalized electromechanical coupling coefficient, K_{ij}, is defined in eq. (42).

For the tuned PMD, the transfer function expression equivalent to eq. (47) is:

$$\frac{x_1}{x_1^{ST}} = \frac{\left(\delta^2 + \gamma^2\right) + \delta^2 r\gamma}{\left(1+\gamma^2\right)\left(\delta^2 + \gamma^2 + \delta^2 r\gamma\right) + \beta\left(\delta^2\gamma^2 + \delta^2 r\gamma^3\right)} \tag{48}$$

with the k_{ij} used in the nondimensionalization set equal to zero and β equal to the damper mass ratio as described in Ref. [15]. By comparing the form of these two equations, (47) and (48), it is evident that the generalized electromechanical coupling coefficient for the tuned piezoelectric case, K_{ij}^2, serves the same function as the mass ratio, β, in the PMD system.

Two techniques for determining the "optimal" tuning criteria will be presented. The first technique parallels the min-max criteria (presented in Ref. [15] for PMDs) for minimizing the maximum of the system transfer function by appropriate choice of the RSP parameters. This technique will be referred to as transfer function optimization, and the optimal parameters will bear the subscript, $()_{TF}$. The second technique will depend on pole placement techniques to choose system pole locations which maximize the magnitude of the real part of the system roots. The optimal parameters using this technique will bear the subscript, $()_{PP}$, to signify pole placement.

Resonant Damper Optimization by Transfer Function Considerations

At this point the optimal tuning parameters using the transfer function technique can be found by duplicating the argument for the PMD [15]. The first step in this process is to find the magnitudes of the transfer functions which correspond to r = zero and r = infinity respectively. From eq. (47) for r = 0:

$$\left|\frac{x_1}{x_1^{ST}}\right|_{r=0} = \left|\frac{\delta^2 - g^2}{(1-g^2)(\delta^2 - g^2) - K_{ij}^2 g^2}\right| \tag{49a}$$

and for r = infinity

$$\left|\frac{x_1}{x_1^{ST}}\right|_{r=\infty} = \left|\frac{1}{(1+K_{ij}^2) - g^2}\right| \tag{49b}$$

These two transfer functions can be equated and a quadratic expression found for the intersection points, called the S and T points in the PMD analysis. This expression is

$$g^4 - g^2\left[\left(1+K_{ij}^2\right) + \delta^2\right] + \left[\frac{\delta^2}{2}\left(2+K_{ij}^2\right)\right] = 0 \tag{50}$$

From the quadratic formula, the sum of the roots of this equation can be found to be

$$g_S^2 + g_T^2 = -\frac{B}{A} = \left(1+K_{ij}^2\right) + \delta^2 \tag{51}$$

Equation (49b) can be solved for the magnitudes at the S and T points. This gives another expression for the sum of the two roots.

$$g_S^2 + g_T^2 = 2\left(1+K_{ij}^2\right) \tag{52}$$

Equating (51) and (52) leads to an expression for the tuning parameter which equalizes the magnitudes of the S and T points. This is the optimum tuning parameter.

$$\delta_{TF}^{opt} = \sqrt{1+K_{ij}^2} \tag{53}$$

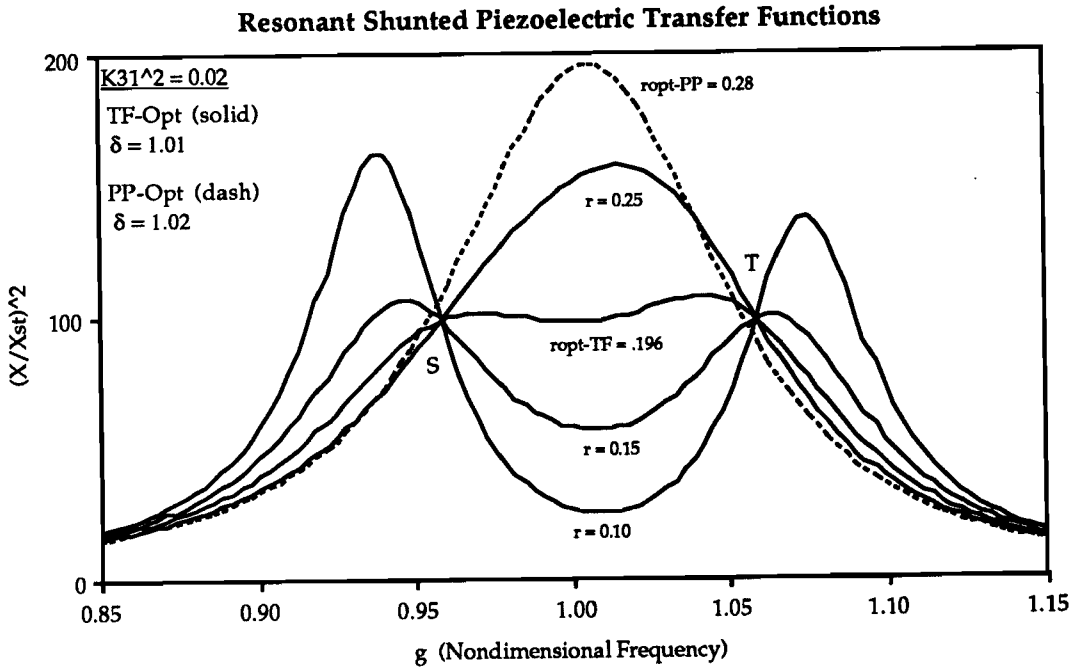

Figure 9: Transfer Function for a Single DOF System Containing a RSP at Various Values of the Damping Parameter,r

Once the optimal tuning has been found using the transfer function criteria, there are several methods for determining the "optimal" damping in the electrical circuit. One method entails setting the amplitude of the system transfer function at a chosen frequency to the amplitude of the transfer function at the invariant frequencies, the S and T points. A particularly convenient (though not technically optimal) frequency corresponds to the electrical tuning at g = δ. The amplitude of the S and T points can be found by first solving equation (50) for the S and T frequencies. The roots of (50) are:

$$g^2_{S,T} = \left(1 + K^2_{ij}\right) \pm \sqrt{\frac{K^2_{ij}\left(1 + K^2_{ij}\right)}{2}} \tag{54}$$

This expression can be substituted into (53) to yield the amplitude at S or T:

$$\left|\frac{x_1}{x_1^{ST}}\right|_{S,T} = \left|\sqrt{\frac{2}{K^2_{ij}\left(1 + K^2_{ij}\right)}}\right| \tag{55}$$

Evaluating the system transfer function, eq. (47), at g = δ and setting this amplitude equal to (55) gives an equation that can be solved for a simple expression for the "optimal" circuit damping:

$$r^{opt}_{TF} \cong \sqrt{2}\frac{K_{ij}}{1 + K^2_{ij}} \tag{56}$$

The subscript, $()_{TF}$, signifies that this expression was derived from transfer function considerations. The effect of various circuit resistor values at optimal tuning is shown in Fig. (9). As can be seen, the system sensitivities to damping parameter variations are essentially identical to the PMD sensitivities. As the damping parameter is increased, the two distinct system modes coalesce into a single mode which converges to the system response with open circuit piezoelectrics as the damping parameter approaches infinity.

Optimal Tuning by Pole Placement Techniques

The second technique for determining the "optimal" tuning parameters is based on s-plane methods described in Ref. [12] for PMDs and outlined in Ref. [9] for piezoelectrics. The s-plane diagram in Fig. (10) shows the root locus for the poles of the shunted piezoelectric system as the damping parameter, r, is varied. Just as in the PMD case, as the damping parameter is increased the distinct poles can coalesce into double complex conjugate pairs *only if* a special value of the frequency tuning parameter, δ, is chossen. This point of coalescence is the point of leftmost excursion in the s-plane. The pole placement method of optimization involves finding the values of the frequency tuning parameter, δ, and the damping parameter, r, which give that point on the s-plane. The poles of the system are found from the denominator of eq. (47). Assuming the coalesced poles are located at the coordinates, $s = a + ib$, $a - ib$, a series of equations for a and b can be found by equating corresponding terms of the characteristic polynomial found in the denominator of eq. (47).

$$\delta^2 r = -4a \tag{57a}$$

$$(1 + \delta^2) + K_{ij}^2 = 6a^2 + 2b^2 \tag{57b}$$

$$\delta^2 r (1 + K_{ij}^2) = -4a(a^2 + b^2) \tag{57c}$$

$$\delta = a^2 + b^2 \tag{57d}$$

These equation can be solved for the parameters, r and δ, to give the value which results in the coalesced poles:

$$\delta_{pp}^{opt} = 1 + K_{ij}^2 \tag{58a}$$

$$r_{PP}^{opt} = 2 \cdot \sqrt{\frac{K_{ij}^2}{\left(1 + K_{ij}^2\right)^3}} = r_{TF}^{opt} \sqrt{\frac{2}{1 + K_{ij}^2}} \tag{58b}$$

The subscript, $()_{pp}$, has been used to signify that the expressions were derived from pole-placement considerations. The transfer function corresponding to optimal tuning and this value of r is shown in Fig. (9). This method tends to give higher steady state responses than the first method presented.

As a practical point the various damper tuning criteria are indistinguishable in all but the most sensitive experimental setups. The ratios given for optimal tuning and electrical damping can now be used to add maximum damping to targeted structural modes. Use of a tuned circuit can increase the structural mode damping several orders of magnitude above simple resistive shunting at the cost of reduced damper bandwidth.

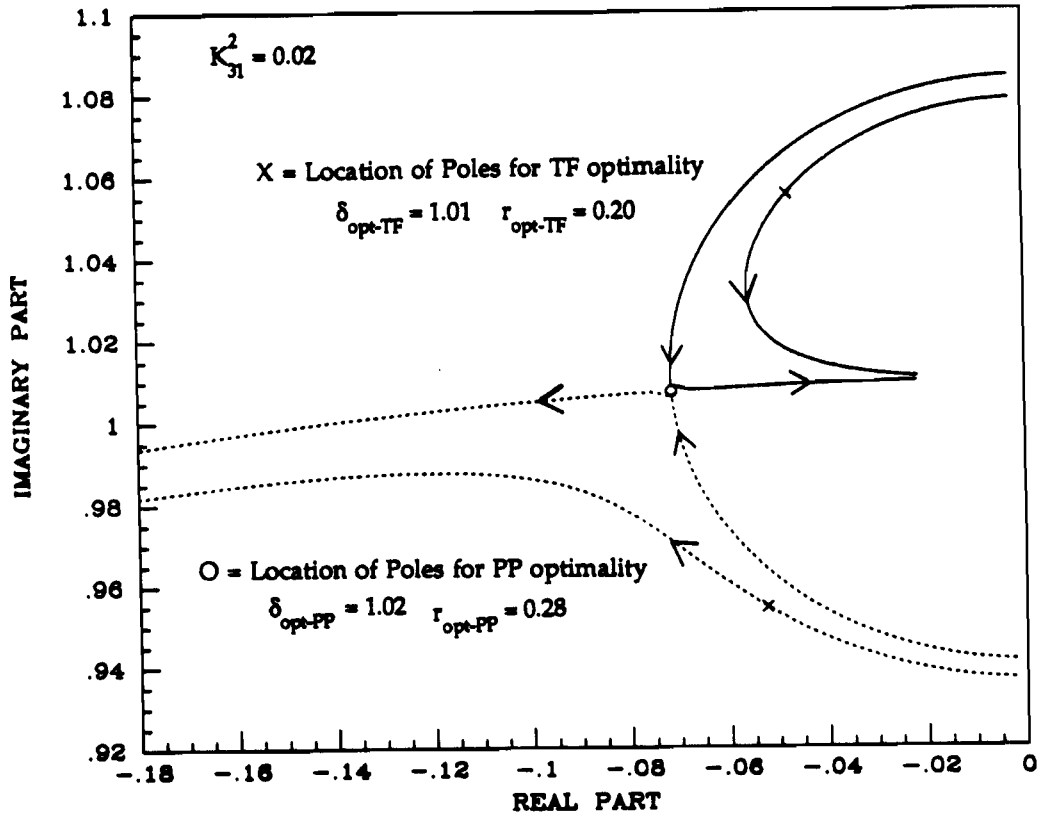

Figure 10: Root Locus for a RSP Damped System at 2 Values of δ as a Function of the Damping Parameter, r, Showing the Pole Locations for the Pole Placement (O) and Transfer Function (X) Optimal Tunings

Summary of Analytical Predictions

For resistive shunted piezoelectrics, the stiffness and loss factor of the piezoelectrics were found to vary with frequency. The loss factor exhibited a maximum at a frequency determined by the shunting resistance and the electromechanical coupling coefficient of the piezoelectric. For common piezoelectric materials this loss factor can be as high as 42.5% for the longitudinal and shear loading cases, and 8% for the transverse loading case. This high loss factor, along with the high stiffness and temperature stability of piezoelectric ceramics, makes them an attractive alternative to viscoelastic materials.

The shunted piezoelectric materials can be modeled within a structural system in two principal ways. They can be modelled as having a frequency dependant complex modulus and incorporated in the same manner as viscoelastic materials. Alternatively, their internal dynamics can be modelled using mechanical impedance and assembled into a system impedance model for dynamic analysis.

For resonant shunted piezoelectrics, the parameters of the resonant circuit can be tuned to a structural mode so as to minimize the maximum response of the mode in a fashion analogous to proof mass damper tuning. The effectiveness of the RSP damper at optimal tuning is dependant on the generalized electromechanical coupling coefficient which is a measure of the percentage of total system modal strain energy actually converted into electrical energy by the piezoelectric. For typical structures where the piezoelectric contains only a small fraction of the structural strain energy, the electrical resonance should be tuned very close to the structural resonance. The optimal damping in the electrical resonance is

also almost linearly dependant on the coupling coefficient in this case. Two sets of tuning criteria are derived, depending on minimizing the magnitude of the transfer function, or minimizing the real part of the system poles.

Description of Experiments

Experiments were conducted to test the validity of the analytical formulae for shunted piezoelectrics. The tests were designed to investigate the properties of the resistive and resonant shunted piezoelectrics.

Dynamic tests were preformed on a cantilevered beam test article with surface bonded piezoceramics and geometry as shown in Fig. (11). The cantilevered beam was 11.53" long, 1.0" wide, and 1/8" thick. Two sets of surface mounted piezoceramics were bonded to the beam. The pair closest to the base was shunted while the pair furthest from the base served to drive the beam. The shunted pair was located 97 mills from the base and extended 2.44". The piezoceramic pairs were separated by 1".

The driving and shunted pairs consisted of 10 mil thick G-1195 piezoceramic sheets manufactures by Piezoelectric Products, Inc. The pairs were poled through their thickness and actuated lengthwise, so that they were operating in the transverse mode. For both pairs, the piezoceramics were attached to the top and bottom surfaces of the beam and wired as shown in Fig. (11), so as to produce a moment on the beam if a voltage were applied as described in Ref. [2]. The piezoceramics are attached to the beam with a very thin layer of conducting epoxy. The beam is grounded and the positive electrodes are attached to the exterior electroded surfaces of the piezoceramic pairs. This produces opposite fields in the top and bottom piezoceramics (which are poled in the same direction), and thus causes the top piezoceramic of a pair to contract as the bottom expands, producing a moment on the beam. Likewise for the shunted pair, a voltage appears across the shunt if the beam is bent. The material properties of the piezoceramics are presented in Table (1). A more detailed discussion of modeling of surface bonded piezoceramics is presented in Ref. [16].

In the shunting experiments, either a resister or a resister and inductor are placed across the piezoelectric electrodes at $Z^{su}(s)$, as shown in Fig. (11). An uncorrelated, pseudo-random voltage is then applied as an input at the positive terminal to excite the beam in the vicinity of its first bending mode at 33 Hz. The white noise excitation signal is produced by a Textronix 2630 data collection system and amplified by a Crown DC-300A audio amplifier. The strain response of the beam is measured at a point 2.74" above the base a shown in Fig. (11). The amplified strain signal is collected by the Tectronix 2630 and a transfer function from input voltage to strain is computed.

In the resistive shunting experiments the shunting resistor is varied over a range of 1/10 to 10 times the theoretical optimum value for maximizing dissipation. Using eq. (38b) the optimum shunting resistance was found to be 28,680 ohms. For each resistance the damping and frequency of the first beam bending mode are identified using a 4^{th} order

Table 1: Piezoelectric Properties of Shunted Piezoceramics

Coupling Coefficient	k_{31}	=	0.35
Elastic Modulus (free)	E^E_{11}	=	63 Gpa
Dielectric Constant	ε^T_3	=	$1700\varepsilon^\circ$
Capacitance (clamped)	C^S_{pi}	=	0.156 μfarad
Curie Temperature		=	360°C

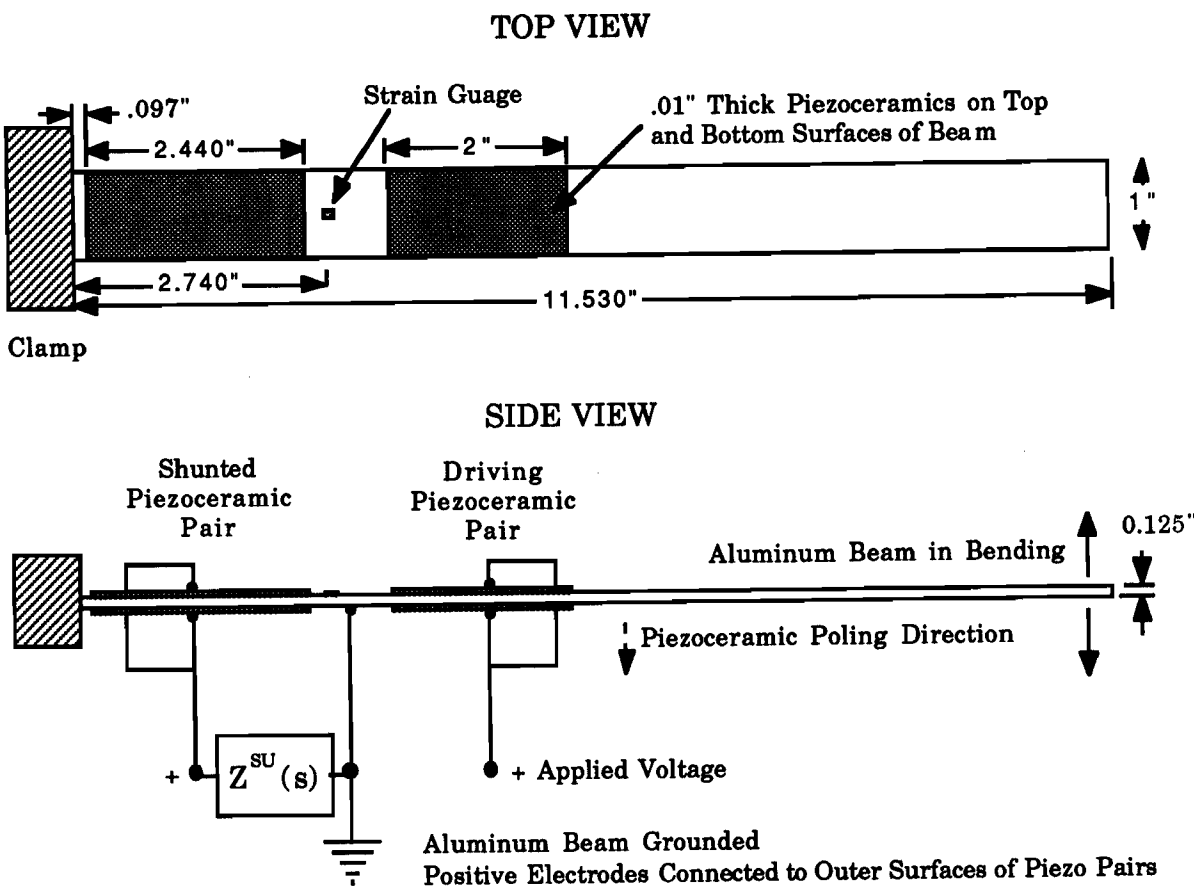

Figure 11: Cantilevered Beam Test Article with Position and Arrangement of Shunted and Driving Piezoceramic Pairs

Recursive Lattice Least Squares (RLLS) algorithm from Ref. [17] applied to the time domain data from which the transfer functions are derived.

For the resonant shunting experiments, a resistor and inductor in series are placed across the piezoelectric leads and the resistor and inductor are tuned to the first beam bending mode, in accordance with eqs. (53) and (56). The transfer function from input current to strain is then measured and compared to the theoretical response for a 1-DOF system derived in eq. (47). The resistance is further varied in the range of the optimal value to validate the behavior of the resonant shunted piezoelectric system in response to parameter changes.

Discussion of Results

The experimental first mode damping for the resister shunting case is shown compared to the analytical predictions in Fig. (12). In this figure, the experimental poles were identified from the random time domain response using the recursive lattice least squares algorithm mentioned previously. The identified damping ratio has been normalized by subtracting off the inherent damping of the beam with the piezoelectrics shorted. The curve thus represents only the damping increase afforded by the shunting process. This is called the experimental added damping.

The two analytical curves were obtained by solving for the roots of the denominator of eq. (40) exactly. The damping ratio was then found from the root location. The upper

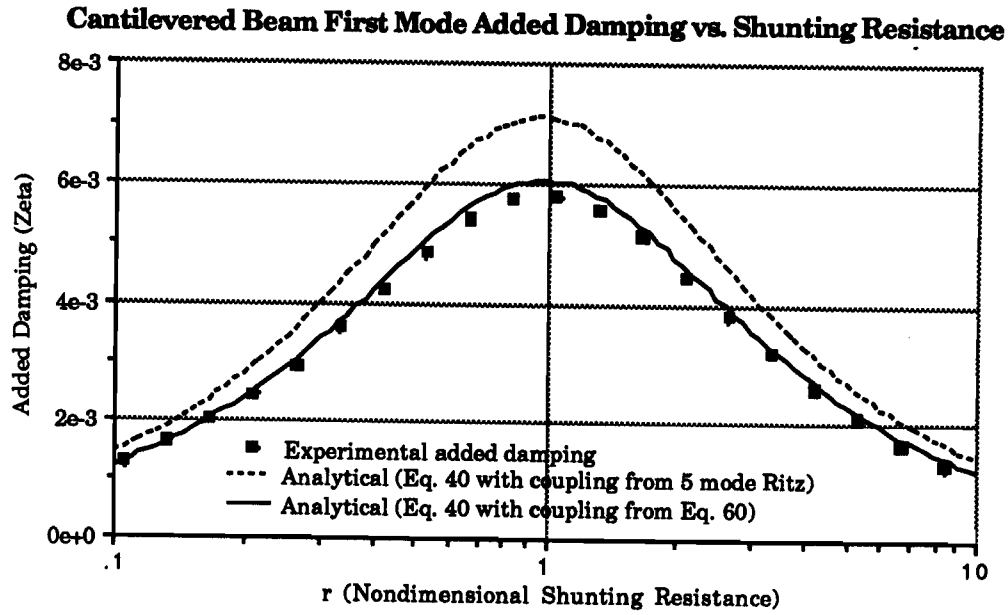

Figure 12: Comparison of Experimental and Analytical First Mode Damping Increase as a Function of the Shunting Resistance

analytical curve reflects the value of the generalized electromechanical coupling coefficient obtained for the shunted piezoceramic pair when a 5 mode Raleigh-Ritz analysis is used to calculate the ratio of strain energy in the piezoelectric to that in the structure, K . For this curve the values of the piezoelectric material properties supplied by the manufacturer were used.

The first five bending modes of a uniform cantilevered beam were used in the 5 mode Ritz model which predicted a first resonant frequency of 35.65 Hz for shorted piezoelectrics and a generalized coupling coefficient, K_{31}, of 0.169. In this analysis, the piezoelectrics were assumed to be perfectly bonded. Details of this type of analysis for bonded or embedded piezoelectrics are presented in Ref. [16]. Since the actual beam had a first natural frequency of 33.36 Hz and the Ritz model accurately represents the system mass, it can be concluded that the Ritz model contains about 14% error in the modal stiffness of the beam. This error will effect the predicted piezoelectric performance. It can be partially accounted for by the finite thickness bond layers of the shunted and driven piezoceramic pairs. The Ritz model thus overestimates the amount of strain energy in the piezoceramic and thus the performance of the resistive shunting.

An alternative approach is to obtain the generalized coupling coefficient by a simple experiment. If it is noted that for a mode of a structure the frequency changes as the stiffness of the piezoelectric changes from its short circuit to open circuit value:

$$\omega_n^E = \sqrt{\frac{K + K_p^E}{M}} \quad and \quad \omega_n^D = \sqrt{\frac{K + \dfrac{K_p^E}{1 - k_{ij}^2}}{M}} \tag{59}$$

then a simple expression for the generalized coupling coefficient for a piezoelectric bonded to a structure can be obtained from the frequency change in these two cases:

$$K_{ij}^2 = \frac{\left(\omega_n^D\right)^2 - \left(\omega_n^E\right)^2}{\left(\omega_n^E\right)^2} \tag{60}$$

The lower analytical curve was obtained by experimentally measuring the first natural frequency of the beam with the shunted pair open or shorted and applying eq. (60) to obtain the generalized electromechanical coupling coefficient. The value obtained was 0.157. This value was then used in the denominator of Eq. (40) and the resulting roots found. As can be seen in Fig. (12), this method exhibits much better agreement with the experimentally determined added damping.

The conclusion of this analysis is that the resistive shunting piezoelectric effect is accurately modelled using the equations presented in this paper, and that the main source of error is in the mechanical models of a piezoelectric bonded to a structure. The experimental curve exhibits the form of the analytical predictions and agrees well with theory once the generalized coupling coefficient has been accurately obtained. For this particular specimen the amount of damping added is not large, because the piezoelectrics store only a small portion of the strain energy and are operating transversely.

The beam transfer functions from applied voltage to strain guage with optimally tuned resonant shunted piezoelectrics are shown compared to the same transfer functions for the beam with shorted or open circuit piezoelectrics in Fig. (13). The change in natural frequency from the shorted to the open circuit piezoelectrics is clear from this figure. The optimal shunting parameter values were calculated from the transfer function criteria (eq. 53 and 56) using the value of the generalized coupling coefficient found from eq. (60). These corresponded to a 142.4 Henry inductor and a 6640 ohm shunting resister. The large inductor was necessary to produce a low electrical resonant frequency.

The resonant shunted piezoelectric pair was found to produce a 35 db drop in peak vibration amplitude from the shorted or open circuit case. This large amplitude reduction is in good agreement with the analytical curves for a 1-DOF system obtained from eq. (47). The experimentally determined natural frequency and base damping of the beam with shorted piezoelectrics were used in the analytical curves as well as the coupling coefficient found by eq. (60). The 1-DOF system curves agrees well in the vicinity of the resonance but fails (as expected) to capture the multiple mode nature of the beam. For this reason the rolloff amplitudes are not identical.

The variation in the beam response as the shunting resister is varied away from the optimal value is presented in Fig. (14) and shown to exhibit tendencies precisely as predicted by the analytical model. This close agreement validates the resonant shunted piezoelectric model. As predicted, the system exhibits two distinct modes when the resister is below its optimal value. As the resistance is increased these modes coalesce into a single mode which converges to the beam response with open circuit piezoelectrics.

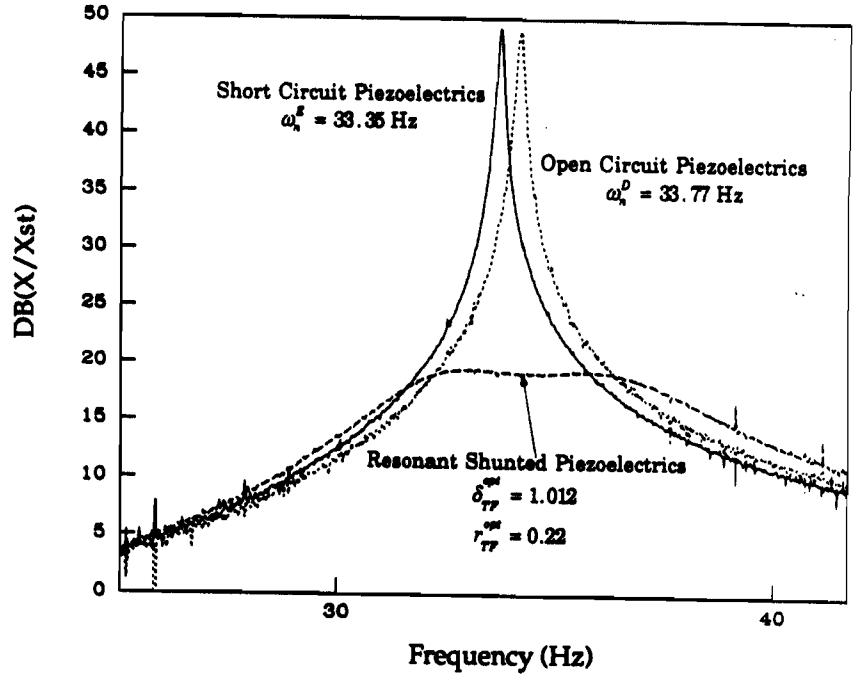

A) Experimental First Mode Transfer Functions with Open Circuit (1), Short Circuit (2), and Optimally Tuned Resonant Shunted Piezoelectrics (3)

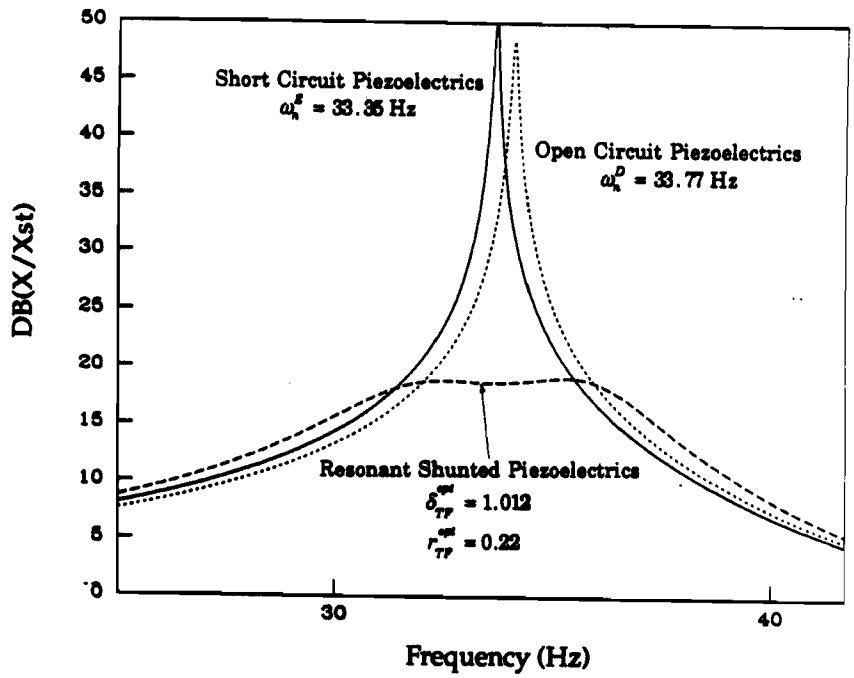

B) Analytical First Mode Transfer Functions with Open Circuit (1), Short Circuit (2), and Optimally Tuned Resonant Shunted Piezoelectrics (3)

Figure 13: First Mode Transfer Functions for Cantilevered Beam with Resonant Shunted Piezoelectric Compared to Beam with Shorted or Open Circuit Piezoelectrics: Experimental (Top) and Analytical (Bottom)

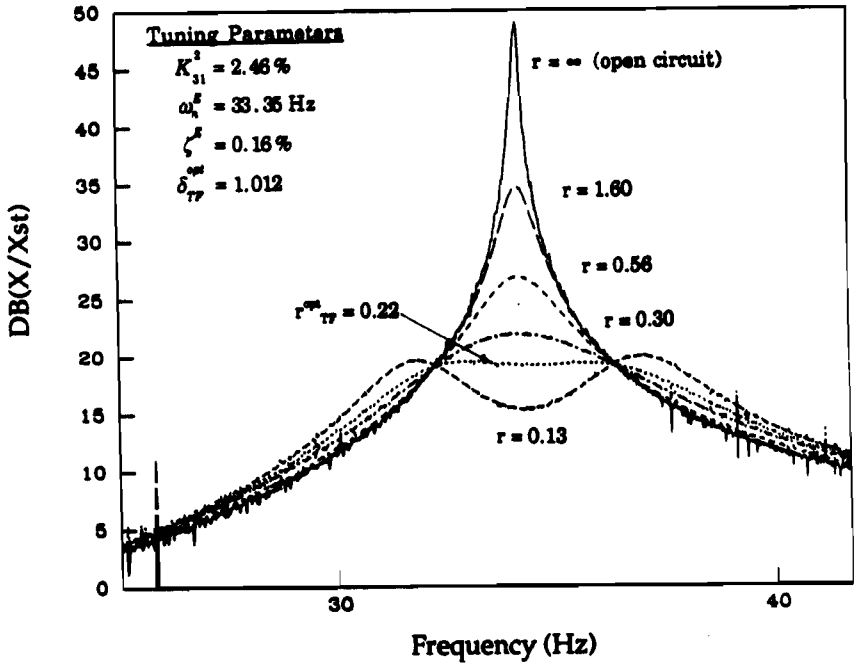

A) Experimental First Mode Transfer Functions with Resonant Shunted Piezoelectrics at Optimal Frequency Tuning and Various Values of the Dissipation Parameter, r

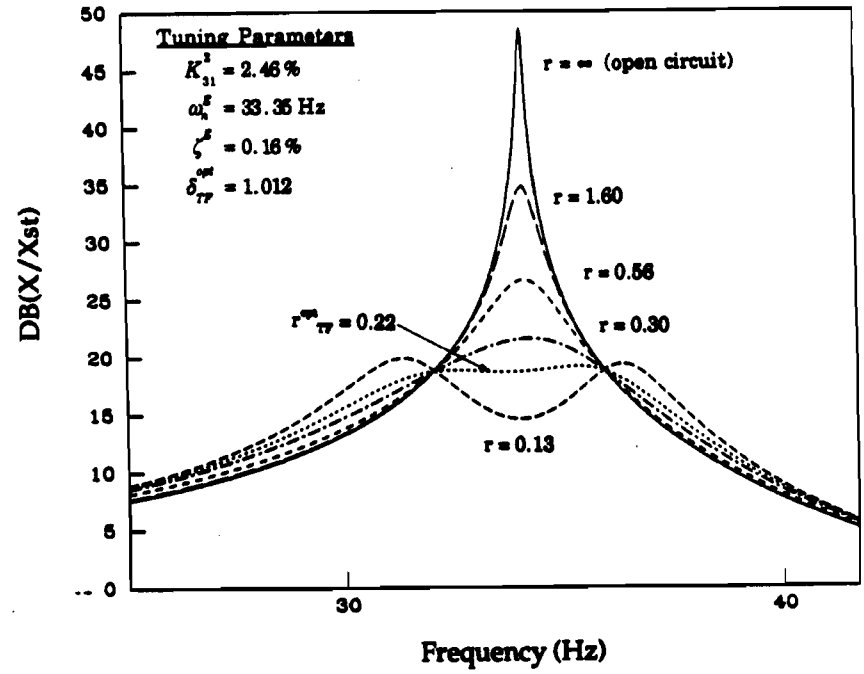

B) Analytical First Mode Transfer Functions with Resonant Shunted Piezoelectrics at Optimal Frequency Tuning and Various Values of the Dissipation Parameter, r

Figure 14: First Mode RSP Dissipation Parameter Variation from r = 0.133 (widely space modes) to r = infinity (open circuit piezoelectrics): Experimental (Top) and Analytical (Bottom)

Conclusions

A new type of structural damping mechanism has been presented based on piezoelectric materials shunted by passive electrical circuits. A model for general shunting of these materials subject ot arbitrary eleastic boundary conditions was developed to determine the 6x6 material compliance matrix when the material is shunted. This model was found to simplify in the case of uniaxial loading and electrical field with the introduction of the material electromechanical coupling coefficient.

The uniaxial equations were then applied to the cases of resistive and resonant circuit shunting. In the resistor shunting case, the optimal shunting resistance for maximizing the piezoelectric material loss factor at a given frequency was determined. The material loss factor was found to be as high as 42% in the longitudinal loading case for commonly available piezoceramics. The high loss factor, together with the high stiffness (63 Gpa) and temperature stability, makes resister shunted piezoelectrics an attractive alternative to viscoelastic materials in structural damping applications.

The problem of determining the global system damping was discussed in the context of the frequency dependant material properties of the piezoceramic, and two techniques were suggested. The shunted piezoelectric elements can be incorporated into the structural stiffness model via a complex modulus representation (like for viscoelastic materials), or analyzed as complex impedances and included in a complex system model (like for electrical systems). Both modelling methods yield identical results. For systems analysis, the energy transfer from the mechanical to electrical parts (and therefore the effectiveness of the shunted piezoelectric) is governed by the generalized electromechanical coupling coefficient which serves as measure of effectiveness. The square of this coefficient represents the ratio of modal strain energy which is converted into electrical energy by the piezoelectric.

Resonant circuit shunting of piezoelectrics was also modelled and shown to exhibit behavior very similar to the well known mechanical tuned vibration absorber. The analogy with the mechanical damper suggested a method of tuning the resonant shunting circuit to a structural mode to optimally damp it. Tuning criteria were developed for the shunting circuit which either minimized the peak amplitude of the system transfer function or placed the poles as far right as possible in the s-plane. The resonant shunting can have large effects on the mode to which it is tuned while the resistor shunting has a larger bandwidth.

Experiments were conducted on a cantilevered beam which validated the shunted piezoelectric models. The models developed were able to accurately predict the influence of the shunted piezoelectrics on the cantilevered beam damping in both the resistive and resonant shunting cases. In both cases, the models also correctly predicted the optimal tuning parameters and effect of variations away from the optimal parameters.

Great benefits for base system energy dissipation can be attained by shunting the electrodes of the piezoelectric material with appropriate passive circuits. The passive shunting introduces damping at the piezoelectric but does not preclude the use of shunted piezoelectrics as actuators in structural active control applications. The analytical models of the shunted piezoelectric, as well as the experimental verification of these models, provides a solid groundwork for future structural damping applications of shunted piezoelectric materials.

Acknowledgements

The authors wish to thank Mr. Walter Chung for his contributions to the experimental phases of this research. This work was sponsored under NASA Grant #NAGW-21 with Mr. Samuel Venneri serving as technical monitor.

References

1. Ashley, Holt; Edberg, Donald L., "On the Virtues and Prospects for Passive Damping in Large Space Structures," Presented at the Air Force Vibration Damping Workshop II, April 1985.
2. Crawley, E. F., deLuis, J., "Use of Piezoelectric Actuators as Elements of Intelligent Structures," AIAA Journal, Vol. 25, No. 10, Oct. 1987, pp.1373-1385.
3. Hagood, Nesbitt W.; Crawley, Edward F., "Development and Experimental Verification of Damping Enhancement Methodologies for Large Space Structures," MIT Space Systems Laboratory Report No. 18-88, September 1988.
4. Hanagud, S.; Obal, M. W.; Calise, A. J., "Optimal Vibration Control by the Use of Piezoceramic Sensors and Actuators," AIAA Paper No. 87-0959, Proc. AIAA S. D. M. Conference, 1987.
5. Bailey, T.; Hubbard, J. E., "Distributed Piezoelectric Polymer Active Vibration Control of a Cantilever Beam," *J. of Guidance and Control*, p. 605, 1985.
6. Pines, Darryll; Flotow, Andreas von, "Active Control of Bending Wave Propagation at Acoustic Frequencies," Proceedings American Control Conference, June 1989.
7. Forward, Robert L., "Electronic Damping of Vibrations in Optical Structures," *Journal of Applied Optics*, Vol. 18, No. 5, March 1979, pp. 690-697.
8. Forward, Robert L., Swigert, C. J., "Electronic Damping of Orthogonal Bending Modes in a Cylindrical Mast- Theory," *Journal of Spacecraft and Rockets*, Vol. 18, Jan. -Feb. 1981, pp. 5-10.
9. Edwards, R. H., Miyakawa, R. H., *Large Structure Damping Task Report*, Hughes Aircraft Co. Report No. 4132.22/1408, May 1980.
10. IEEE Std 176-1978, "IEEE Standard on Piezoelectricity,", 1978, pp. 9 - 14.
11. Jaffe, B.; Cook, R.; Jaffe, H., *Piezoelectric Ceramics*, Academic Press, New York, NY., 1971.
12. Miller, David W.; Crawley, Edward F., "Theoretical and Experimental Investigation of Space-Realizable Inertial Actuation for Passive and Active Structural Control," J. Guidance Control and Dynamics, Vol. 11, No. 5, Sept-Oct 1988, pp.449-458.
13. Hagood, Nesbitt W., Crawley, Edward E., "A Frequency Domain Analysis for Damped Space Structures," 30th AIAA/ASME/ASCE/AHS Structures, Structural Dynamics, and Materials Conference, April 1989, AIAA Paper No. 89-1381.
14. Nasif, Ahid D.; Jones, David I. G.; Henderson, John P., *Vibration Damping*, John Wiley & Sons, New York, 1985, pp.69-73.
15. Timoshenko, Stephen; Young, D.H.; Weaver, W., Jr., *Vibration Problems in Engineering*, 4th Ed., John Wiley and Sons, New York, 1974.
16. Anderson, E. H., Crawley, E. F., "Detailed Models of Piezoceramic Actuation of Beams," 30th AIAA/ASME/ASCE/AHS Structures, Structural Dynamics, and Materials Conference, April 1989, AIAA Paper No. 89-1388.
17. Lee, Daniel T.L.; Morf, Martin; Friedlander, Benjamin, "Recursive Least Squares Ladder Estimation Algorithms" IEEE Transactions on Acoustics, Speech and Signal Processing, Vol. ASSP 29, No. 3, June 1981, pp. 627-641.